THE JOURNAL OF PHYSICAL CHEMISTRY C

Article

pubs.acs.org/JPCC

Novel Si Networks in the Ca/Si Phase Diagram under Pressure

Guoying Gao,[†] N. W. Ashcroft,[‡] Maosheng Miao,[§,∥] and Roald Hoffmann*[,†]

[†]Department of Chemistry and Chemical Biology, Cornell University, Ithaca, New York 14853, United States

[‡]Laboratory of Atomic and Solid State Physics, Cornell University, Ithaca, New York 14853, United States

[§]Beijing Computational Science Research Center, Beijing 100084, China

[∥]Materials Research Laboratory, University of California Santa Barbara, Santa Barbara, California 93106-5050, United States

Supporting Information

ABSTRACT: The rich Ca/Si binary phase diagram is explored here theoretically and over a range of pressures, through four stoichiometries: Ca_2Si, CaSi, $CaSi_2$, and $CaSi_3$. The calculations are calibrated by recovering the known P = 1 atm structures (even as they suggest metastable alternatives for some) and by predicting correctly the range of pressures at which $CaSi_3$, which has a positive heat of formation at P = 1 atm, can be synthesized. Ca_2Si, in accord with its Zintl compound nature, features isolated Si^{4-} ions then chains until decomposition. CaSi, which begins as a Zintl phase (albeit metallic) chain structure evolves to rings and zeolitic-channel structures, while $CaSi_2$ explores a variety of triply connected Si polytypes to Laves phases with increasing pressure. $CaSi_3$ has a calculated narrow range of stability of 8−18 GPa. Interestingly, all the phases studied are calculated to decompose to the elements at $P \sim 250$ GPa. This unusual behavior is traced to the special compressibility of elemental Ca and the backward charge transfer from Si to Ca. All the phases studied are metallic, except that Ca_2Si is a semiconductor at 1 atm.

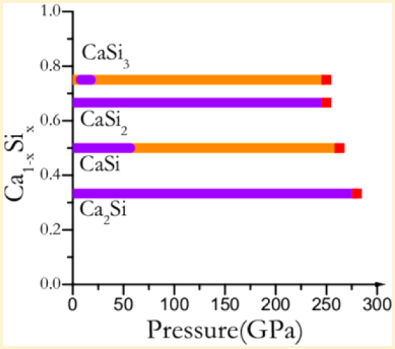

1. INTRODUCTION

On the way to a study of the Ca/Si/C phase diagram, we found that we needed a thorough understanding of the Ca/Si binary system. Compounds of calcium and silicon are hardly new; they have been the object of extensive investigation since 1863. At P = 1 atm, a number of different stable compositions are known, including Ca_2Si, Ca_5Si_3, CaSi, Ca_3Si_4, $Ca_{14}Si_{19}$, and $CaSi_2$. At 10−15 GPa and in the temperature range 900−1500 K, $CaSi_3$[1] and $CaSi_6$[2] have also been synthesized; $CaSi_3$ can be returned to P = 1 atm, but $CaSi_6$ cannot. No evidence of more calcium-rich compounds than Ca_2Si has been obtained; indeed, in an ionic formulation Ca_2Si is the natural limit, seen as $(Ca^{2+})_2Si^{4-}$. On the Si-rich side there appears to be no such constraint on the stoichiometries possible. In this work we therefore explore theoretically a representative portion of the Ca/Si phase diagram, concentrating on Ca_2Si, CaSi, $CaSi_2$, and $CaSi_3$ as representative examples.

The first reliable crystallographic data for Ca_2Si were those of Eckerlin and Woller,[3] who reported a $PbCl_2$-type cell (Figure 1a). This was later confirmed by Manfrinetti but given a revised name, *anti*-$PbCl_2$.[4] In this structure, Si occurs as isolated Si^{4-} ions. The 1:1 composition, CaSi, crystallizes in the orthorhombic CrB-type structure, space group *Cmcm*.[5,6] In CaSi (Figure 1b), the Si atoms form buckled Si^{2-} chains.

At 1 atm and room temperature $CaSi_2$ adopts a rhombohedral structure[7] (space group *R*-3*m*, usually labeled *TR*6), in which corrugated Si^- hexagonal layers alternate with Ca hexagonal layers along the [001] direction, and both layers stack in an *AA′BB′CC′* sequence (Figure 1c). Rhombohedral

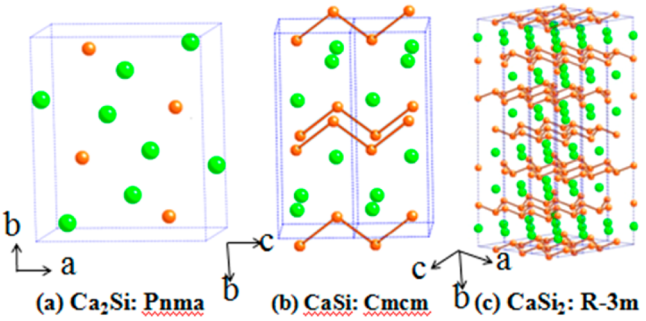

Figure 1. Known structures for Ca_2Si (a), CaSi (b), and $CaSi_2$ (c) at P = 1 atm. Here (and throughout the paper), Ca's are depicted as large green spheres and Si's as smaller orange ones.

$CaSi_2$ is a semimetal, but not a superconductor, down to temperatures as low as 30 mK.[8]

The observed P = 1 atm structures of Ca_2Si, CaSi, and $CaSi_2$ can be understood on the basis of the simple and useful Zintl idea: transfer electrons from the electropositive element, then form covalent bonds, if possible, in the anionic framework.[9] Thus, in Ca_2Si, Si^{4-} cannot form Si−Si bonds; the Si ions remain isolated. In CaSi, the Si^{2-} ion can be viewed as a diradical, and the −Si−Si−Si− chains observed are one resolution of the bonding situation. In $CaSi_2$, each Si is

Received: August 2, 2014
Revised: October 3, 2014
Published: October 6, 2014

formally Si^{-}, capable of forming three bonds. As we will see, there are a number of ways to satisfy this structural requirement; the observed structure is one of these. The C_2^{2-} units in CaC_2 indicate another way, forming triple bonds between two carbons, $Ca^{2+}(C_2)^{2-}$. We will eventually see other possibilities.

Pressure gives us another variable, one that enriches the structural chemistry of compounds. The discussion to follow will give details, but briefly what we know is the following: $CaSi_2$ transforms to a tetragonal phase at 5.76 GPa and 783 K, one showing superconductivity, with T_c rising from 1.58 K at 1 atm up to 6.5 K at 9 GPa. This phase is a high-T, high-P phase. As the pressure is increased at room temperature, two other phases follow, whose T_c values reach a still higher value, up to 14 K. No experimental information appears to be available on the conductivity of compressed Ca_2Si and CaSi. CaSi is metallic at 1 atm, a point to which we will return.

In this work, we examine the structural possibilities for Ca_2Si, CaSi, $CaSi_2$, and $CaSi_3$ over the pressure range of 1 atm to 400 GPa. We predict upon compression a number of interesting stable or metastable Si networks in the four calcium silicides studied. Our calculations indicate that Si atoms will form Si_n linear chains in Ca_2Si, flat quadrangular and hexagonal Si layers in CaSi, and triply coordinated Si polytypes and Laves phases in $CaSi_2$ at high pressure. We will see and explain an instability of all phases to the elements at ∼250 GPa.

2. COMPUTATIONAL METHODS

We searched for Ca_2Si, CaSi, $CaSi_2$, and $CaSi_3$ ground-state and high-pressure structures using Crystal structure AnaLYsis by Particle Swarm Optimization methodology, as implemented in the CALYPSO code.[10,11] We performed structure searches with system sizes containing up to eight formula units (f.u.) per simulation cell. Each generation contains 30 structures, 60% of which are generated by particle swarm optimization and the others by random choice. We followed 30−50 generations (depending on the size of the system) to achieve the converged structure.

The underlying *ab initio* structural relaxations were carried out with density functional theory using the Perdew−Burke−Ernzerhof (PBE)[12] exchange-correlation functional as implemented in the VASP code.[13] The frozen-core all-electron projector-augmented wave method was adopted,[14] with $3s^23p^64s^2$ (cutoff radius $2.3a_0$) and $3s^23p^2$ (cutoff radius $1.9a_0$) treated as valence electrons for Ca and Si, respectively. The pseudopotentials have been tested by reproducing the Fermi surface for pure fcc-Ca[15] and the band gap for diamond-Si at 1 atm, respectively. Thus, the experimental band gap for diamond-Si is 1.17 eV; our calculated value is 0.6 eV with the PBE functional, improving to 1.0 eV with an HSE hybrid functional. An energy cutoff of 600 eV and appropriate Monkhorst−Pack[16] (MP) k meshes were chosen to ensure that enthalpy calculations were well converged to better than 1 meV/formula unit (f.u.). The phonon calculations were carried out by using a supercell[17] approach within the PHONOPY code.[18]

3. RESULTS AND DISCUSSION

3.1. Ca_2Si: Isolated Ions and Chains. The experimentally known *anti*-$PbCl_2$ (*Pnma*) structure (Figure 2a) for Ca_2Si at 1 atm is successfully reproduced by our crystal structural searches. Our calculated lattice constants at 1 atm are also consistent with the experimental data (see Table S1 in the Supporting Information (SI) to this paper), which provide a check on the reliability of the calculations that follow. In this phase silicon exists as a Si^{4-} ion, as we discussed above: the closest Si−Si separation is 4.62 Å, much longer than a 2.35 Å Si−Si bond length, as in diamond-type silicon at the same pressure.

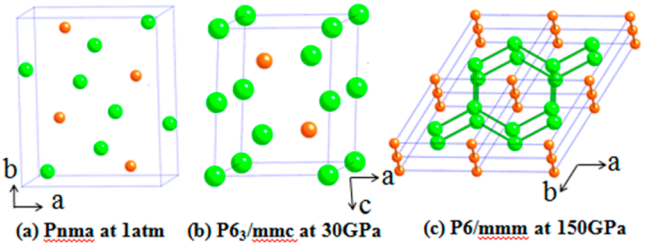

Figure 2. Various predicted ground-state static structures for Ca_2Si. The lines connecting the Ca ions in (c) are just a guide to the eye, no bonding is implied.

As we increase the pressure, another structure acquires a lower enthalpy, a hexagonal close-packed $P6_3/mmc$ phase (Figure 2b). The Si atoms remain isolated and separated from adjacent Si atoms by 3.97 Å at 30 GPa and 3.79 Å at 50 GPa. This structure is a derivate of the AlB_2 structure, with one Ca atom and a Si atom together forming graphitic layers (at z = 0.25 and 0.75) that sandwich the other kind of Ca atoms (at z = 0 and 0.5). As the pressure is increased, an *anti*-AlB_2 structure, $P6/mmm$ (Figure 2c), becomes stable beyond 50 GPa. In this structure, the graphitic layers are exclusively formed by Ca atoms. The Si atoms in different layers form linear Si chains, where the nearest-neighbor Si−Si separations at 150 GPa, i.e., the vertical separations in Figure 2c, are 2.27 Å, just a little longer than the 1.96 Å in *Fd*-3*m* (diamond-type) Si at the same pressure.[19] Figure S1 in the SI shows the calculated Si−Si separations in diamond-type Si over a range of pressures; they serve as a calibration on the Si−Si separations obtained throughout our paper.

Starting with these candidate structures, we reoptimized them over a range of pressures, obtaining the enthalpy curves of Figure 3. The low-pressure predicted $P6_3/mmc$ structure is the reference. At 1 atm, the *anti*-$PbCl_2$ (*Pnma*) structure is the most stable one; it transforms to the $P6_3/mmc$ structure when a relatively low pressure of ∼10 GPa is applied. Then, over a very wide pressure range between 40 and 280 GPa, the *anti*-AlB_2 $P6/mmm$ phase is preferred. We also calculated the enthalpy of the elements, thereby providing an estimate of the heat of formation of Ca_2Si. The SI shows several possible decompositions to the elements; the preferred separated element phases change with pressure. Figure 3 shows only a curve for decomposition to the high P forms of Ca and Si. Clearly, above 280 GPa Ca_2Si becomes unstable with respect to disproportionation into separated elements. This is unusual, and it will turn out to be a consistent feature of the behavior of Ca/Si phases under pressure.

3.2. CaSi: Chains, Rings, and Zeolitic Channel Structures. For static ground-state CaSi, at 1 atm, we find that the CrB-type *Cmcm* structure (Figure 4a) is the most stable enthalpically, which is in good agreement with the experimental findings for this stoichiometry.[5,6] Our calculated lattice constants for *Cmcm*-CaSi at 1 atm (see SI) are again consistent with the experimental data. However, at 20 GPa, a

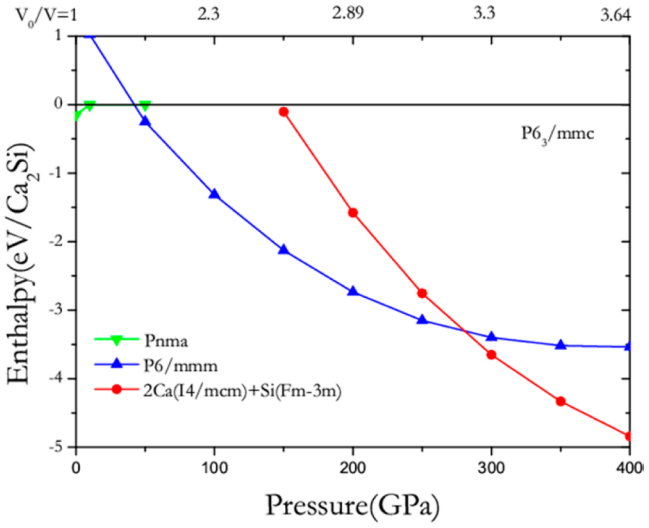

Figure 3. Ground-state static enthalpy curves per formula unit as a function of pressure for Ca_2Si, with respect to the predicted $P6_3/mmc$ structure. The decomposition enthalpies for Ca_2Si to Ca + Si are also presented. We considered the $I4/mcm$ structure for separated pure solid Ca and $Fm\bar{3}m$ for Si. The relative compression (V_0/V) is again indicated at the top.

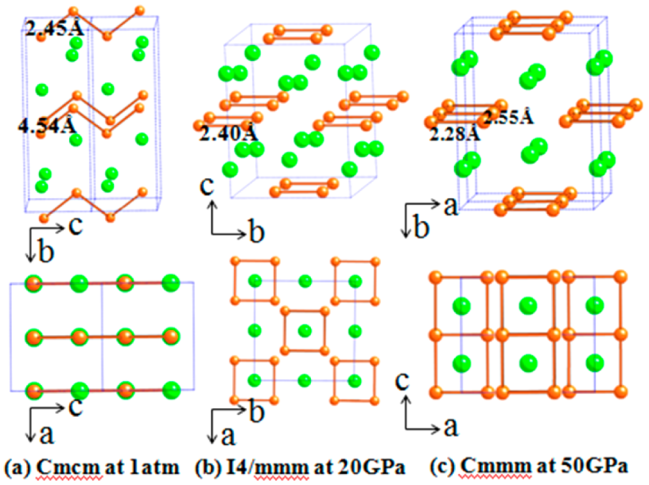

Figure 4. Various predicted ground-state static structures for CaSi. The lower panels show projections along *b*, *c*, and *b*, respectively, of the corresponding structures in the upper panels.

new tetragonal $I4/mmm$ structure (Figure 4b) is preferred; it consists of layers of Si_4 squares alternating with Ca layers.

The Zintl picture of Si in CaSi as Si^{2-} provides the opportunity for each Si to form two bonds. This may be satisfied by infinite chain formation, as in the *Cmcm* structure, or by forming rings. Thus, one could imagine alternatives with the Si^{2-} centers condensing to give dimers $(Si{=}Si)^{4-}$ or cyclic trimers, tetramers, pentamers, etc. The $I4/mmm$ structure, with its Si_4 squares, is one such choice. It is stable in the region 12–50 GPa. Note the Si–Si separation in the $I4/mmm$ structure (2.40 Å) is not far from that expected for a calculated Si–Si single bond (2.245 Å at 20 GPa) in pure solid diamond-type Si (Figure S1, SI). Zintl phases, in a sense being an extension of the kind of bonding one finds in molecules obeying the octet rule, would be expected to be semiconducting. CaSi is not. An excellent recent study of CaSi by Kurylyshyn et al. explains the metallic character of CaSi and shows the limits of the Zintl model in describing this solid.[20]

At 50 GPa, the adjacent Si_4 squares in the same layer begin to bond to each other and form flat ladders, so the $I4/mmm$ structure transforms to *Cmmm* (Figure 4c). The projections along *b*, *c*, and *b* directions, respectively, make this evolution clear.

A very different and interesting metastable hexagonal $P6/mmm$ structure evolves at elevated pressures (Figure 5). In this

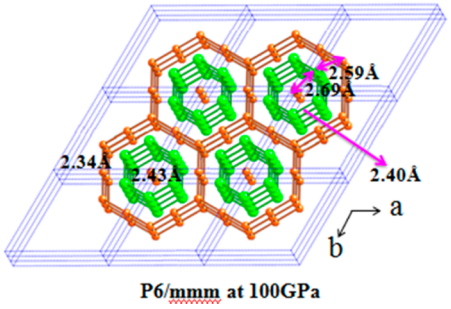

Figure 5. Predicted ground-state static structure for CaSi at 100 GPa. The symmetry is $P6/mmm$.

unusual phase, 12 Si atoms in each plane form a large hexagon, and each hexagon is bonded to another six hexagons. Judging from the Si–Si separations (2.43 Å), the Si atoms in different layers are also bonded to each other, forming clear channels. For comparison, the Si–Si separation in diamond Si at 100 GPa is 2.04 Å (Figure S1, SI). Every six Ca atoms above and below the Si layers also form small hexagons (Ca–Ca, 2.40 Å), which are also bonded to each other in different layers (Ca–Ca, 2.43 Å) but not bonded within the same layer (shortest Ca–Ca, 3.96 Å). For comparison the Ca–Ca separation in metallic Ca (*Cmca*) is 3.38 Å at 1 atm and 2.29 Å at 100 GPa. Although the small Ca hexagons and the large Si hexagons are not in the same layer, they share the same center, which, remarkably, is occupied by a linear Si chain, with Si–Si separations of 2.43 Å. A zeolitic-type framework thus evolves, featuring Si lines inside Ca tubes, inside channeled Si networks. In this hexagonal structure, Si atoms are 2-, 4-, and 5-fold coordinated.

It should be emphasized that this interesting structure is not at any pressure the most stable CaSi phase. It is nevertheless dynamically stable, which is why we mention it.

Phases evolve rapidly in this system, as the pressure rises, *Cmcm* → $I4/mmm$ → *Cmmm*. Figure 6, the calculated ground static enthalpy per CaSi, shows that overall the range of stability of CaSi is quite limited. In the pressure range of 57–263 GPa, CaSi is unstable with respect to disproportionation to Ca_2Si + $CaSi_2$. Then, above 263 GPa, CaSi becomes unstable to decomposition to its constituent elements.

3.3. $CaSi_2$. Experimentally, $CaSi_2$ at P = 1 atm and ~300 K is known in two closely related $R\text{-}3m$ structures ($hR3$ and $hR6$; one is shown in Figure 7a). These structures are polytypes, differing only by a registry shift of the Si hexagonal layers. At 5.7 GPa and 783 K,[21] $CaSi_2$ transforms to a tetragonal (α-$ThSi_2$-type) phase (space group $I4_1/amd$, Figure 7b) in which the Si atoms are connected by a three-dimensional network of sp^2 bonds. Tetragonal $I4_1/amd$-$CaSi_2$ can be quenched to 1 atm and room temperature and is a superconductor with T_c = 1.58 K.[22] Moreover, T_c rises to 6.5 K when one compresses tetragonal $CaSi_2$ to 9 GPa.

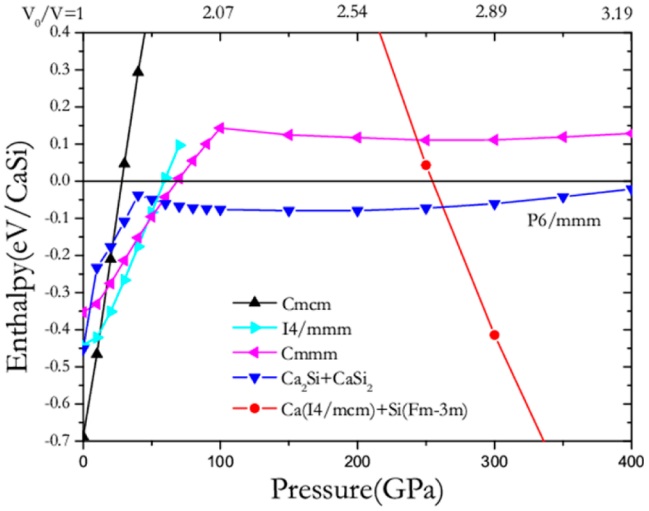

Figure 6. Ground-state static enthalpy curves for CaSi as a function of pressure, with respect to the reference enthalpy for the predicted *P6/mmm* structure. The decomposition enthalpies for CaSi to Ca + Si are also presented. We considered the *I4/mcm* structure for separated pure solid Ca and $Fm\bar{3}m$ for Si. The relative compression (V_0/V) is also indicated at the top of the figure.

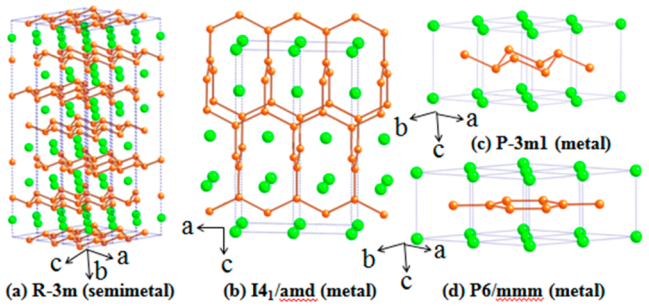

Figure 7. Various known ground-state static structures for $CaSi_2$ at low pressure.

The $CaSi_2$ system shows remarkable structural variety. At 7.6 GPa and room temperature, $CaSi_2$ is stable in still another trigonal structure (space group *P*-3*m*1, Figure 7c) in which corrugated Si hexagonal layers also alternate with Ca hexagonal layers along the [001] direction, but both layers (SiSi and CaCa) stack in a simple *AA* sequence.[21,23] The *P*-3*m*1 structure is still another polytype of *R*-3*m*, the $P = 1$ atm structure. Finally, at 16 GPa and room temperature, a new phase is found experimentally. It can also be optimized in *P*-3*m*1 symmetry but with a significant increase of the Si z (in $(0,0,z)$) parameter from ~0.4 to ~0.44, which leads to a strong decrease of the Si layer buckling (the largest vertical distance from the bottom to the top atom in the same buckled layer) from 0.7 to 0.4 Å. This phase can also be described as close to a higher symmetry $EuGe_2/AlB_2$-type structure (*P6/mmm*, Figure 7d), and for which $z \sim 0.5$.[24] However, this $EuGe_2/AlB_2$-type structure is not quenchable.

Note that all of these structures contain triply connected Si networks, as the Zintl ideas would imply for Si^-. Interestingly, the high-pressure *P*-3*m*1 and AlB_2-type structures are both superconductors; the T_c measured can reach as high as 14 K,[24] which is the highest T_c reported so far for a disilicide, almost 1 order of magnitude higher than those found in other silicides, and comparable to the T_c's of the A-15 compounds.[24]

Our $P = 1$ atm, ground-state static calculations reproduced the two *R*-3*m* structures with the lowest enthalpy (Figure 8).

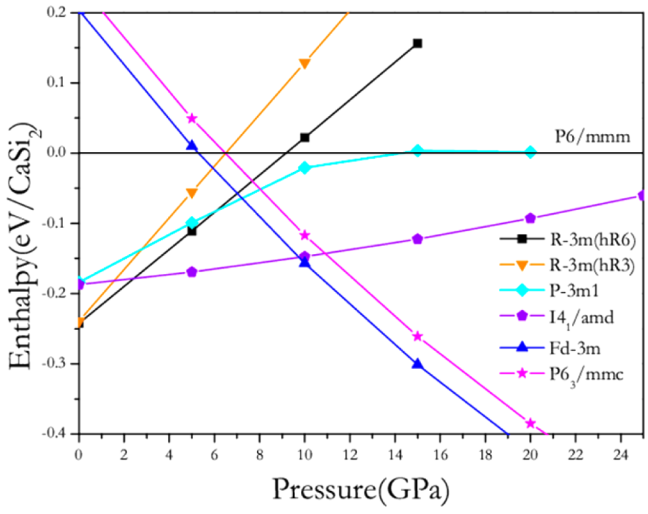

Figure 8. Ground-state static enthalpy curves per formula unit for $CaSi_2$ at relatively low pressures, with respect to that for the *P6/mmm* structure.

Less than 50 meV/$CaSi_2$ above these, we predicted the $I4_1/amd$ structure found experimentally at slightly higher pressure and elevated T and the *P*-3*m*1 structure found experimentally at higher pressure and room temperature. We thus see at least four structures available for $CaSi_2$ at $P = 1$ atm, all within 0.06 eV/formula unit of each other. The zero-point energies calculated in the harmonic approximation for the *R*-3*m* structure are 0.132 eV/$CaSi_2$ and are very similar for the other three structures (e.g., 0.127 eV/$CaSi_2$ for the *P*-3*m*1 phase). So they will not change the rough stability order of these phases.

The $I4_1/amd$ structure becomes most stable between 3 and 10 GPa. The most stable ground-state structure we find above 10 GPa is quite different from the four structures mentioned; it is a cubic Laves phase structure ($MgCu_2$ type) and also a face-centered-cubic (fcc) $BaAl_2$-type structure, space group *Fd*-3*m* (Figure 9a). The *Fd*-3*m* structure remains most stable at 50, 100, and 200 GPa, respectively. This is a very interesting metallic structure; in it we see perfect tetrahedra (nearest neighbor Si−Si separations of 2.27 Å) at 100 GPa (diamond-type Si at this pressure would have a Si−Si separation of 2.04 Å see Figure S1, SI), and each tetrahedron shares a vertex with

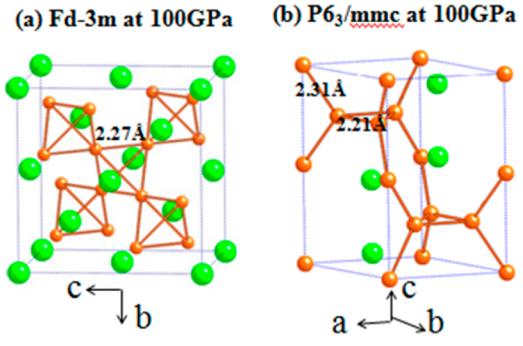

Figure 9. Predicted ground-state static $Fd\bar{3}m$ (a) and $P6_3/mmc$ (b) structures for $CaSi_2$ at high pressure.

four adjacent tetrahedra.[25−27] The centers of tetrahedra occupy half of the tetrahedral (T) holes of the fcc structure formed by Ca atoms, while the other Ca atoms occupy the other half T sites. Each Si atom is then equidistant from six other Si atoms.

At all pressures, another hexagonal Laves phase ($MgZn_2$ type: $P6_3/mmc$, Figure 9b) is remarkably close in enthalpy to the cubic Fd-3m one (see Figure 8 for P < 25 GPa and Figure 10 for higher pressures). In this structure, each Si atom has

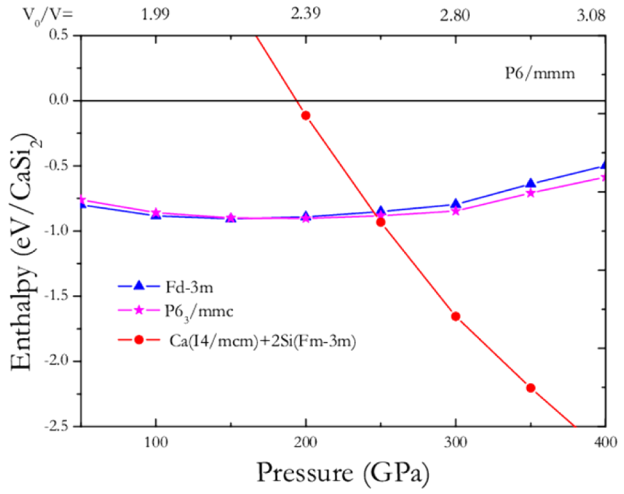

Figure 10. Ground-state static enthalpy curves per formula unit as a function of pressure for $CaSi_2$, with respect to that for the $P6/mmm$ structure. Only the high-pressure region is shown; for low P see Figure 9. The decomposition enthalpies for $CaSi_2$ to Ca + Si are also presented. We considered $I4/mcm$ for separated pure solid Ca and $Fm\bar{3}m$ for Si. The relative compression (V_0/V) is also shown.

coordination number 6, and the Si−Si separations—2.21 and 2.31 Å at 100 GPa—are very close to those in Fd-3m $CaSi_2$ but a little longer than the separation in pure diamond-type Si at the same pressure (Figure S1, SI). The very similar Si−Si separations and the Laves phases formed in both Fd-3m and $P6_3/mmc$ structures for $CaSi_2$ are likely responsible for their very similar stability over a very wide pressure range. Both of the two Laves phases are dynamically stable at 1 atm, which contrasts to the recent report on the high-pressure synthesis of $CaSi_{2-x}Al_x$ ($CuAl_2$ type). These authors were not able to synthesize the phase for x = 2, and the highest Si content was around x = 1.5.[28]

Near 250 GPa, several new structures emerge as metastable, as shown in the SI. However, it is also at this approximate pressure that $CaSi_2$, like Ca_2Si and CaSi, becomes unstable relative to the separated elements.

3.4. $CaSi_3$: Stable Only in a Narrow Pressure Range. $CaSi_3$ has been synthesized from $CaSi_2$ and Si at pressures between 12 and 15 GPa and temperatures from 900 to 1400 K and then returned to P = 1 atm.[1] One way to describe the crystal structure, $I4/mmm$, is to see in it two Si_2 pairs (Si−Si separations of 2.39 and 2.40 Å see Figure 11), connected by clearly bonding interactions (Si−Si separations of 2.58 and 2.68 Å). Our ground-state static calculations at 1 atm reproduced this $I4/mmm$ structure as metastable. We also found three metastable phases at slightly lower enthalpy at P = 1 atm; their structures are shown in the SI. These contain alternate puckered graphitic Si and diamond-like layers with Ca in between; the main difference between them is the number of layers. One way to think about these $CaSi_3$ networks is to

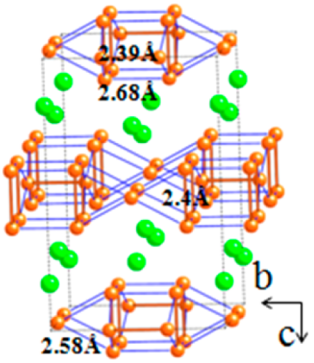

Figure 11. Ground-state static structure for $CaSi_3$ at 1 atm.

imagine Ca intercalated in a diamond Si net and then transferring two electrons per three Si to the net. These would enter Si−Si antibonding orbitals, breaking some bonds in the diamond Si structure.

At 50 GPa and at higher pressures we found a number of fascinating metastable structures featuring Kagome nets and a $AuCu_3$ structure. However, at all pressures other than just around 10 GPa the $CaSi_3$ structures are unstable relative to decomposition to $CaSi_2$ and Si, and above ∼250 GPa $CaSi_3$ is calculated to decompose into the elements, just as we found for the other Ca/Si phases studied. The SI shows and discusses the metastable $CaSi_3$ phases.

Figure 12 shows the simplified version of the enthalpy relationships as the pressure is raised for $CaSi_3$; the full diagram,

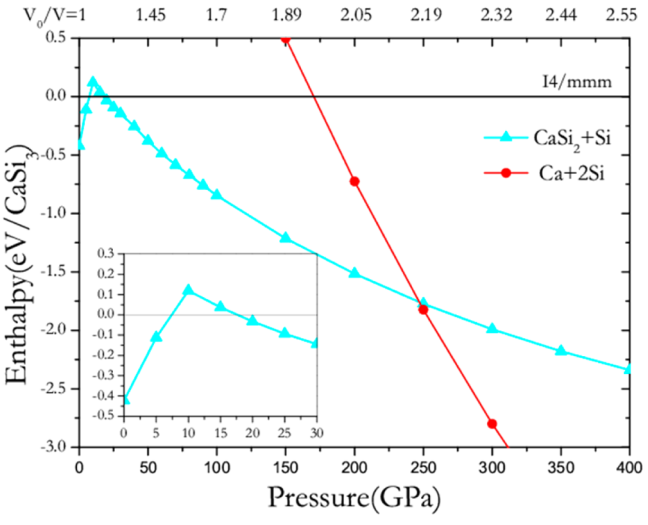

Figure 12. Ground-state static enthalpy (per formula unit) curves as a function of pressure for $CaSi_3$, with respect to that for the observed $I4/mmm$ structure at 12−15 GPa and 900−1400 K. The decomposition enthalpies for $CaSi_3$ to $CaSi_2$ + Si and Ca + Si are also presented. We considered $I4/mcm$ for pure solid Ca and the most stable forms for $CaSi_2$ and Si at the corresponding pressure. The inset shows the enthalpy (eV) vs pressure (GPa) in the low-pressure regime, so as to indicate more clearly the limited region of $CaSi_3$ stability.

including metastables, is in SI. The important point here is that the synthesis of $CaSi_3$ was not an accident. As our calculations show, synthesis requires access to a rather precisely circumscribed pressure range around 10 GPa.

3.5. Formation Enthalpies. To compare the relative stabilities of different stoichiometries for the $CaSi_x$ series, we

examine the enthalpy tie-line graphs (Figure 13). The reference line is pure Ca and Si, each in its most stable form at the

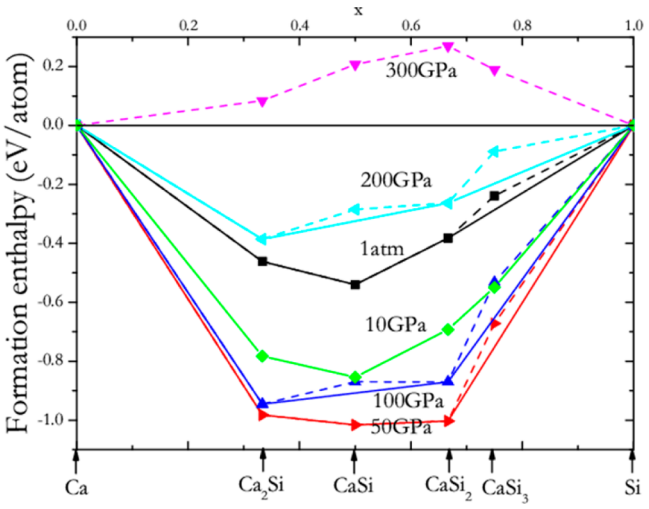

Figure 13. Ground-state and static enthalpy of formation per atom of the $Ca_{(1-x)}Si_x$ phases with respect to their separated counterparts; calcium molar content (x = 0 corresponds to pure calcium; x = 1 to pure silicon) for the ground state and P = 1 atm to 10, 50, 100, 200, and 300 GPa. The symbols on the solid line mark those calcium silicides that are stable at the corresponding pressure, while those on the dashed line refer to calcium silicides that are unstable with respect to disproportionation into other calcium silicides and calcium or silicon.

pressures specified. Note that, at 1 atm, Ca_2Si, CaSi, and $CaSi_2$ are all stable with respect to dissociation into the elements, while $CaSi_3$ is calculated as metastable and is predicted to decompose into $CaSi_2$ and Si, as the previous section detailed. As pressure increases, the formation enthalpy for Ca_2Si, CaSi, and $CaSi_2$ decreases; maximum stability is reached around 50 GPa. Above this pressure, the formation enthalpy for all the stoichiometries becomes less and less negative and finally changes to positive; i.e., the compounds become in our calculations unstable with respect to decomposition into the elements above ~250 GPa. During this process, CaSi first becomes metastable above 100 GPa, unstable with respect to Ca_2Si and $CaSi_2$. As discussed above, $CaSi_3$ is stable only in a narrow pressure range of 8−18 GPa.

Figure 14 summarizes in another way the stability ranges for each stoichiometry studied. Note again the conclusion that all phases in this system are unstable relative to the elements *above* a pressure of ~250 GPa. Let us next discuss and try to rationalize this phenomenon.

3.6. Reasons for the Decomposition to the Elements at High Pressure. In our computations, every Ca/Si phase becomes enthalpically unstable with respect to the elements at a pressure of around 250−280 GPa. This uniform behavior is not something we have encountered before in our previous studies of materials under pressure. However, it has been observed (theoretically) for some other systems, among them CH_4,[29] $CaLi_2$,[30,31] ZnX,[32] CdX,[33] and HgX[32] (X = S, Se, or Te).

Let us focus on one system, Ca_2Si, whose enthalpy in various structures is shown in Figure 3. In Figure 15 we show the energy and PV contributions to the enthalpy difference of the elements relative to Ca_2Si. The elements and the compound are each chosen to be in their most stable form at the pressure indicated.

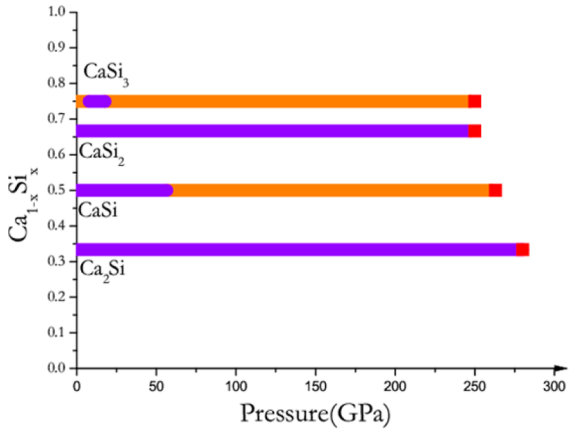

Figure 14. Ground-state static binary $Ca_{(1-x)}Si_x$ phase stability ranges as a function of pressure. Purple lines denote stable pressure ranges. The red symbols indicate the initial pressure at which the compound becomes unstable with respect to the elements.

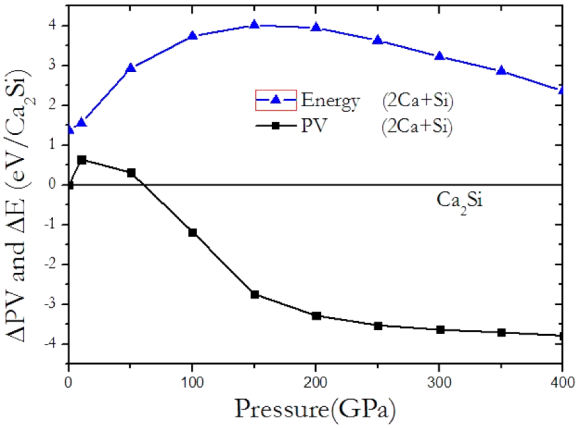

Figure 15. Ground-state energy and PV components of the enthalphy of the elements relative to Ca_2Si.

One notices immediately that while both energy and PV terms favor compound formation at relatively low pressures the ΔPV term quickly grows negative and accordingly makes ΔH negative overall at around 250 GPa. In other words, the specific volumes of Ca and Si decrease faster than that of their compound.[34]

Is the effect attributable to Ca or to Si? Figure 16 shows the compression ratios for the elements as a function of pressure. Clearly Ca is far more compressible than Si; the former element's compressibility is among the highest of the metallic elements, approaching that of Li.

The ease with which Ca is compressed has firm electronic origins. It has been known for some time that under moderate pressure Ca switches from being a mainly s-like metal to a transition-metal-like d metal.[35−37] Electrons in Ca bands that are mainly 3d-like are quite compressible, as there is no inner d-like core to which the electronic wave functions need be orthogonal.

In a recent study of high-pressure electrides[38] we found useful a simple model in which atoms are compressed in a helium lattice. Figure 17 shows the energies of Ca 4s, Ca 3d, and Si 3p orbitals in such a model compression chamber.

Aside from the aforementioned 4s to 3d switch for Ca under 25 GPa, we observe in Figure 17 that the energy of compressed Ca 3d electrons approaches that of Si 3p as the pressure

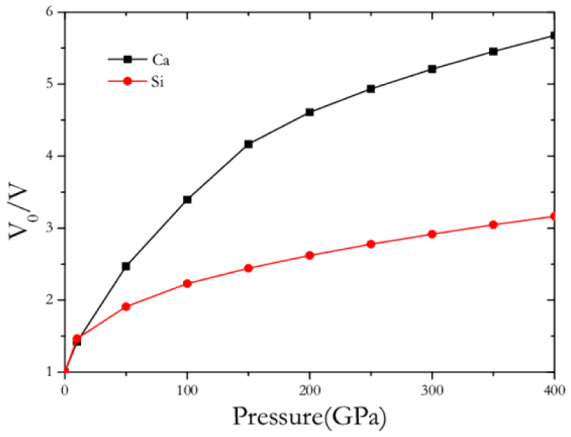

Figure 16. Compressibility, V_0/V, for Ca and Si.

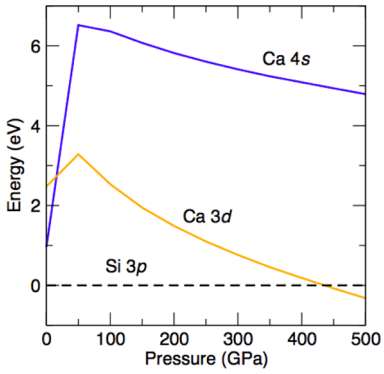

Figure 17. Energies of various Ca and Si atomic orbitals in a 107-atom helium compression model; Si 3p is the reference.

increases. We now see in this a suggestion of increased propensity for covalent Si−Ca bonding. Since the attractive interaction between Ca and Si in the stable stoichiometries that form is primarily ionic, the growth-of-covalence/decrease-of-ionicity with pressure should discriminate energetically against the compound. We confirm the decrease in ionicity with pressure by looking at the respective charges in a Quantum Theory of Atoms in Molecules (QTAIM) analysis[39] (see SI). Also in the SI is a demonstration of the increasing Ca−Si covalence by examination of the integrated Crystal Orbital Hamilton Populations (COHP) values[40] for the respective bonds.

The above considerations are supported by what Figure 15 shows—the internal energy of the elements begins to turn down (relative to the compound) with increasing pressure. The favoring of the elements arises in largest part from the ΔPV term, but eventually ΔE begins to contribute.

The details of our argument were given here for Ca_2Si. An examination of the other stoichiometries shows similar effects, with ΔPV favoring the elements and producing eventually, as the pressure increases, a positive heat of formation.

3.7. Dynamical Stability. The calculated phonon spectra for metastable or stable phases of each stoichiometry within its enthalpy stability range show no imaginary frequencies, indicating that these structures are dynamically stable. The computational results are given in the SI. Moreover, we found that certain high-pressure phases, such as *I*4/*mmm*-CaSi, *Fd*-3*m*, $P6_3/mmc$-$CaSi_2$, and *I*4/*mmm*-$CaSi_3$, are also calculated to be dynamically stable at 1 atm. This points to a possible synthesis of these phases, by pressurization and also a possible return to P = 1 atm. Indeed as we mentioned, *I*4/*mmm*-$CaSi_3$ has already been synthesized in just this way.

3.8. Electronic Properties. The calculated electronic density of states (DOS) per valence electron for static *Pnma*-Ca_2Si, *Cmcm*-CaSi, *R*-3*m*-$CaSi_2$, and *R*3*m*-$CaSi_3$ at 1 atm is shown in the SI. Ca_2Si is a semiconductor, as expected from its structure and the Zintl picture—it contains weakly interacting Si^{4-} ions. CaSi, with its characteristic Si−Si bonded chains, might also be expected to have a gap, but clearly it is metallic. Through an analysis of experimental charge densities as well as theory, Kyrylyshyn et al.[20] showed that the chemical bonding in CaSi may be described from a Zintl starting point but needed to be supplemented by highly polar Si → Ca σ donation and somewhat weaker Si → Ca π donation components. The partial covalent character of the Ca−Si bonds appears be the physical origin of the remarkable metallicity of CaSi. Both $CaSi_2$ and $CaSi_3$ are metallic at 1 atm.

When we compress them to 50 GPa, *P*6/*mmm*-Ca_2Si, *P*6/*mmm*-CaSi, *Fd*-3*m*-$CaSi_2$, and *P*-4*m*2-$CaSi_3$, each stoichiometry in its most stable structure (see previous sections), are all calculated to be metals (Figure 18). An analysis of the contributions of various atomic orbitals to the total electronic DOS indicates that the electronic DOS at the Fermi level has important contributions both from the Ca 3d and Si 3p orbitals.

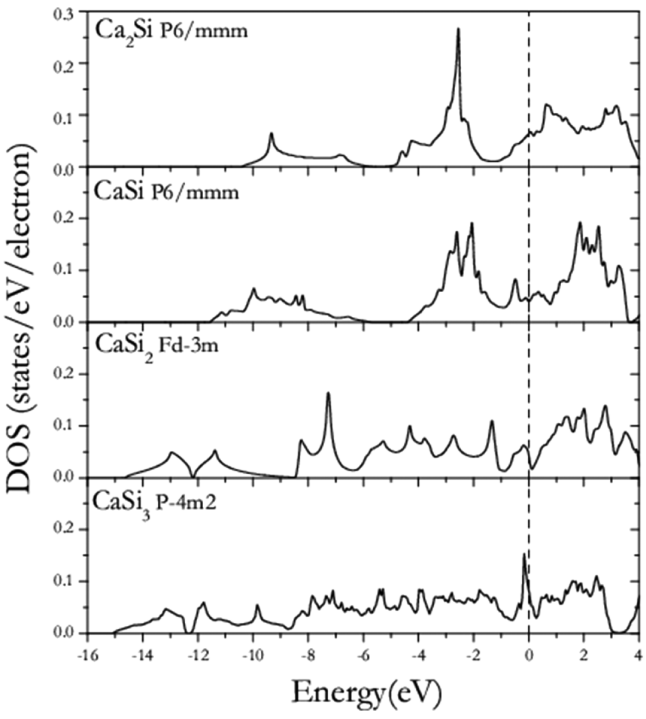

Figure 18. Density of states (DOS) per valence electron of Ca_2Si, CaSi, $CaSi_2$, and $CaSi_3$ at 50 GPa. The vertical dashed line locates the Fermi energy. It is clear that all of these calcium silicides are metallic.

Considering that $CaSi_2$ at low pressure is a superconductor with T_c up to 14 K below 20 GPa and that the calcium silicides studied are all metallic under high pressure, we did explore in some detail the superconductivity of CaSi and $CaSi_2$ over a range of pressure. The details are provided in the SI. There is reasonable agreement with experiment where it is known and with preceding calculations, but the estimated T_c of all phases is never high.

4. CONCLUSIONS

We have explored systematically the ground-state phases of selected calcium silicides under pressure. Our computations confirm that Ca_2Si, CaSi, and $CaSi_2$ are the stable stoichiometries at 1 atm, while $CaSi_3$ is metastable. Under pressure, Ca_2Si, CaSi, and $CaSi_2$ are further stabilized up to about 50 GPa, while $CaSi_3$ reaches stability only in a very narrow pressure range of 8−18 GPa. This is in agreement with the way $CaSi_3$ was synthesized. At 1 atm, Si atoms exist as isolated Si^{4-} ions in Ca_2Si, form chains in CaSi, puckered six-membered rings in $CaSi_2$, and Si_2 pairs in metastable $CaSi_3$. Under pressure, we found many novel and interesting Si networks—chains in Ca_2Si, flat four-memebered rings and channels in CaSi, and Lave phases in $CaSi_2$. All the phases studied in this system become unstable relative to the elements above a pressure of ∼250 GPa. We traced this unusual phenomenon to the special compressibility of Ca as a consequence of an s to d electron switch and to backward charge transfer from Si to Ca.

All of the calcium silicides studied are dynamically stable, and also metallic, except that Ca_2Si is a semiconductor at 1 atm.

■ ASSOCIATED CONTENT

Supporting Information

Computational methods, other predicted structures for certain stoichiometries, phonon spectra, total density of states, electron−phonon coupling, and structural information. This material is available free of charge via the Internet at http://pubs.acs.org.

■ AUTHOR INFORMATION

Corresponding Author

*E-mail: rh34@cornell.edu.

Author Contributions

All authors have given approval to the final version of the manuscript.

Notes

The authors declare no competing financial interest.

■ ACKNOWLEDGMENTS

We thank Accelrys Inc. for making available to us their Materials Studio software which we have used in our computations. G.G., R.H., and N.W.A. acknowledge support by the National Science Foundation, through research grant CHE-1305872 and DMR-0907425, and also EFree, an Energy Frontier Research Center funded by the U.S. Department of Energy (Award No. DESC0001057 at Cornell). Computational resources provided in part by Efree and the XSEDE network (provided by the National Center for Supercomputer Applications through grant TG-DMR060055N). We are also grateful to a reviewer for very useful suggestions.

■ REFERENCES

(1) Schwarz, U.; Wosylus, A.; Rosner, H.; Schnelle, W.; Ormeci, A.; Meier, K.; Baranov, A.; Nicklas, M.; Leipe, S.; Muller, C. J.; et al. Dumbbells of five-connected silicon atoms and superconductivity in the binary silicides MSi_3 (M = Ca, Y, Lu). *J. Am. Chem. Soc.* **2012**, *134*, 13558−13561.

(2) Wosylus, A.; Prots, Y.; Burkhardt, U.; Schnelle, W.; Schwarz, U. High-pressure synthesis of the electron-excess compound $CaSi_6$. *Sci. Technol. Adv. Mater.* **2007**, *8*, 383−388.

(3) Eckerlin, P.; Woller, E. Die Kristallstruktur von Ca_2Si und Ca_2Ge. *Z. Anorg. Allg. Chemie. Bd.* **1955**, *280*, 321−331.

(4) Manfrinetti, P.; Fornasini, M. L.; Palenzona, A. The phase diagram of the Ca-Si system. *Intermetallics* **2000**, *8*, 223−228.

(5) Rieger, W.; Parthé, E. Bond lengths in bis-salicylaldoximato-nickel. *Acta Crystallogr.* **1967**, *22*, 919−922.

(6) Currao, A.; Curda, J.; Nesper, R. Kann man die Arten von Zintl-Anionen steuern? Variationen uber das Thema Si2- im System Sr/Mg/Si. *Z. Anorg. Allg. Chem.* **1996**, *622*, 85−94.

(7) Pearson, W. B. *Handbook of Lattice Spacing and Structures of Metals and Alloys*; Pergamon: New York, 1958.

(8) Affronte, M.; Laborde, O.; Olcese, G. L.; Palenzona, A. Low temperature properties of calcium mono- and disilicides. *J. Alloys Compd.* **1998**, *274*, 68−73.

(9) Fässler, T. F. *Zintl Phases: Principles and Recent Developments, Book Series*: Structure and Bonding; Springer: Heidelberg, 2011.

(10) Wang, Y.; Lv, J.; Zhu, L.; Ma, Y. Crystal structure prediction via particle-swarm optimization. *Phys. Rev. B* **2010**, *82*, 094116.

(11) Wang, Y.; Lv, J.; Zhu, L.; Ma, Y. CALYPSO: A method for crystal structure prediction. *Comput. Phys. Commun.* **2012**, *183*, 2063−2070. http://www.calypso.org.cn.

(12) Perdew, J. P.; Burke, K.; Ernzerhof, M. Generalized Gradient Approximation Made Simple. *Phys. Rev. Lett.* **1996**, *77*, 3865.

(13) Kresse, G.; Furthmüler, J. Efficient iterative schemes for ab initio total-energy calculations using a plane-wave basis set. *Phys. Rev. B* **1996**, *54*, 11169.

(14) Blöchl, P. E. Projector augmented-wave method. *Phys. Rev. B* **1994**, *50*, 17953.

(15) Rasolt, M. Pressure effects on the electronic properties of Ca, *Ph.D. thesis*, June 1971.

(16) Monkhorst, H. J.; Pack, J. D. Special points for Brillouin-zone integrations. *Phys. Rev. B* **1976**, *13*, 5188.

(17) Parlinski, K.; Li, Z. Q.; Kawazoe, Y. First-Principles Determination of the Soft Mode in Cubic ZrO_2. *Phys. Rev. Lett.* **1997**, *78*, 4063.

(18) Togo, A.; Oba, F.; Tanaka, I. First-principles calculations of the ferroelastic transition between rutile-type and $CaCl_2$-type SiO_2 at high pressures. *Phys. Rev. B* **2008**, *78*, 134106.

(19) This is a theoretical value; elemental Si undergoes a series of phase transitions to other structures as the pressure is increased.

(20) Kurylyshyn, I. M.; Fassler, T. F.; Fischer, A.; Hauf, C.; Eickerling, G.; Presnitz, M.; Scherer, W. Probing the Zintl−Klemm Concept: A Combined Experimental and Theoretical Charge Density Study of the Zintl Phase CaSi. *Angew. Chem., Int. Ed.* **2014**, *53*, 3029−3032.

(21) Imai, M.; Kikegawa, T. Phase Transitions of Alkaline-Earth-Metal Disilicides $M_{AE}Si_2$ (M_{AE} = Ca, Sr, and Ba) at High Pressures and High Temperatures. *Chem. Mater.* **2003**, *15*, 2543−2551.

(22) Evers, J. Transformation of Three-Connected Silicon Nets in $CaSi_2$. *J. Solid State Chem.* **1979**, *28*, 369−377.

(23) Bordet, P.; Affronte, M.; Sanfilippo, S.; Nunez-Regueiro, M.; Laborde, O.; Olcese, G. L.; Palenzona, A.; LeFloch, S.; Levy, D.; Hanfland, M. Structural phase transitions in $CaSi_2$ under high pressure. *Phys. Rev. B* **2000**, *62*, 11392−11397.

(24) Sanfilippo, S.; Elsinger, H.; Nunez-Regueiro, M.; Laborde, O.; LeFloch, S.; Affronte, M.; Olcese, G. L.; Palenzona, A. Superconducting high pressure $CaSi_2$ phase with T_c up to 14 K. *Phys. Rev. B* **2000**, *61*, R3800−R3803.

(25) Actually, such isolated (and somewhat distorted) tetrahedra have been found in the crystal structures of KSi, RbSi, and CsSi.

(26) von Schnering, H. G.; Schwarz, M.; Chang, J.-H.; Peters, K.; Peters, E.-M.; Nesper, R. *Z. Kristallogr. New Struct.* **2005**, *220*, 525−527.

(27) Evers, J.; Oehlinger, G.; Sextl, G.; Weiss, A. Hochdruck-Phasen von KSi, KGe, RbSi, RbGe, CsSi und CsGe im NaPb-Typ. *Angew. Chem.* **1984**, *96*, 512−513.

(28) Tanaka, M.; Zhang, S.; Inumaru, K.; Yamanaka, S. High-Pressure Synthesis and Superconductivity of the Laves Phase Compound $Ca(Al,Si)_2$ Composed of Truncated Tetrahedral Cages $Ca@(Al,Si)_{12}$. *Inorg. Chem.* **2013**, *52*, 6039.

(29) Gao, G. Y.; Oganov, A. R.; Ma, Y. M.; Wang, H.; Li, P. F.; Li, Y. W.; Litaka, T.; Zou, G. T. Dissociation of methane under high pressure. *J. Chem. Phys.* **2010**, *133*, 144508.
(30) Tse, J. S.; Klug, D. D.; Desgreniers, S.; Smith, J. S.; Dutrisac, R. Instability of $CaLi_2$ at high pressure: Theoretical prediction and experimental results. *Europhys. Lett.* **2009**, *86*, 56001.
(31) Xie, Y.; Oganov, A. R.; Ma, Y. M. Novel High Pressure Structures and Superconductivity of $CaLi_2$. *Phys. Rev. Lett.* **2010**, *104*, 177005.
(32) Li, Z. W.; Wang, H. B.; Li, Y.; Ma, Y. M.; Cui, T.; Zou, G. T. Pressure-induced elemental dissociation in zinc Chalcogenides. *New J. Phys.* **2010**, *12*, 043058.
(33) Ma, Y.M., Private communication.
(34) A similar explanation has been suggested to us by Ma, Y., private communication, by email, 3/29/2014.
(35) Maksimov, E. G.; Magnitskaya, M. V.; Fortov, V. E. Non-simple behavior of simple metals at high pressure. *Phys.-Usp.* **2005**, *48*, 761−780.
(36) Gao, G. Y.; Xie, Y.; Cui, T.; Ma, Y. M.; Zhang, L. J.; Zou, G. T. Electronic structures, lattice dynamics, and electron−phonon coupling of simple cubic Ca under pressure. *Solid State Commun.* **2008**, *146*, 181−185.
(37) Oganov, A. R.; Ma, Y.; Xu, Y.; Bergara, A.; Lyakhov, A. O. Exotic behavior and crystal structures of calcium under pressure. *Proc. Natl. Acad. Sci. U.S.A.* **2010**, *107*, 7646−7651.
(38) Miao, M. S.; Hoffmann, R. High Pressure Electrides: A Predictive Chemical and Physical Theory. *Acc. Chem. Res.* **2014**, *47*, 1311−1317.
(39) Bader, R. *Atoms in Molecules: A Quantum Theory*; Oxford Univ. Press: Oxford, U.K., 1990.
(40) Dronskowski, R.; Blochl, P. E. Crystal orbital Hamilton populations (COHP): energy-resolved visualization of chemical bonding in solids based on density-functional calculations. *J. Phys. Chem.* **1993**, *97*, 8617−8624.